2020 IEEE/RSJ International Conference on Intelligent Robots and Systems (IROS)
October 25-29, 2020, Las Vegas, NV, USA (Virtual)

Human-Drone Interaction for Aerially Manipulated Drilling using Haptic Feedback

Dongbin Kim and Paul Y. Oh

***Abstract*— This paper presents a concept for haptic-based human-in-the-loop aerial manipulation for drilling. The concept serves as a case study for designing the human-drone interface to remotely drill with a mobile-manipulating drone. The notion of the work stems from using drones to perform dangerous tasks like material assembly, sensor insertion while being vertically elevated from bridge, wind turbine, and power line. Presented is the aerial manipulator, the customized haptic drill press, the gantry-based test-and-evaluation platform design, material drilling results in the gantry, and validation-and-verification results for indoor flight trials.**

I. INTRODUCTION

In the past decade, aerial manipulation has been implemented for operations such as valve-turning [1], structure assembly [2], and package manipulation [3][4], and industrial applications [5]-[7]. Because such vehicles are free-floating, the challenges mainly involve counter-balancing the reaction forces and torques generated from the manipulator-object interaction. The fundamentals for aerial manipulation are also theoretically understood [8]. The critical gap to complete implementation and hence adoption, stems from autonomy.

Autonomous aerial manipulation of objects that are complex-shaped or when their properties are not known *a priori*, remains an open research question. Relaxing the constraint on autonomy may simplify manipulation but still have value. For example, most robotic surgery is not autonomous and requires human skill and yet accelerates procedures. This paper thus raises questions on the designs for human-in-the-loop aerial manipulation. The motivation for this paper is that such designs could augment those working on dangerous tasks while vertically lifted or suspended from a bridge, wind turbine blade, or power line.

Haptic-based interfaces are employed in medical robots, mobile phones, virtual reality (VR), and wearable devices. Such interfaces are used for robot surgery, touch screens, interactive controllers, and clinical rehabilitation respectively [9]-[12]. In aerial manipulation, haptic integration could provide important feedback for tasks such as valve-turning, sensor insertion, and object pick-and-place. Toward this vision, the authors recently presented a testing-and-evaluation platform for collaborative aerial manipulation [13]. The notion of the work is that the worker performing the task can leverage the haptic feedback assessment of object properties to collaboratively perform manipulation using drones. This could yield collaborative drones that augment a worker's ability to perform assessment and maintenance remotely. The platform was designed in a gantry-based system with a commercial haptic device. The flight trials validated and verified efficacy of this platform.

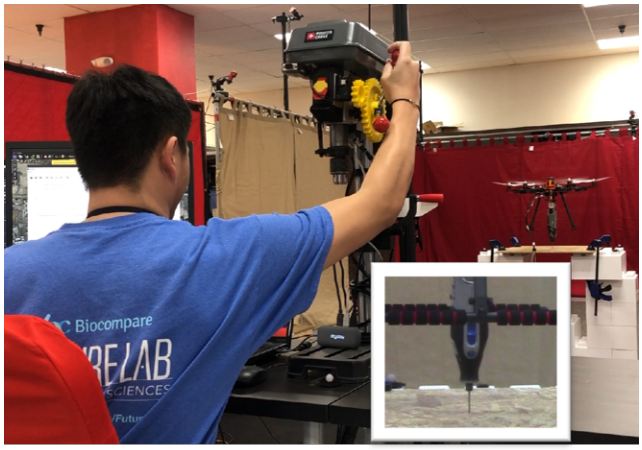

Fig. 1: Aerial manipulation with a customized haptic drill press. Operator feels reaction forces on the manipulator (inset); Inset shows a rotary drill manipulator drill pressing on a plywood board

This paper presents a concept for haptic-based human-in-the-loop aerial manipulation to remotely work on surfaces. This concept stems from the authors collaborative project with the US Department of Transportation (DOT) for bridge maintenance, inspection and repair. Surfaces like the decks and bottoms of bridges often need prep work like drilling pilot holes. Drones have the potential to relieve workers from being suspended from cranes or lifted by scissor jacks. People generally use their sense of touch when drilling. Hence this paper explores haptic-based human-in-the-loop aerial drilling. This serves as a case study for designing the human-drone interface to remotely drill with a mobile-manipulating drone. Aerial manipulation in [14][15], have demonstrated such tasks for sensor insertion and material drilling. However in these works, the operators were not involved in the manipulation loop. Additionally, object properties were assessed after flight operations. In such tasks, haptic assessment could enable the operator-in-the-loop to inspect material condition and increase task dexterity. Figure 1 demonstrates the overall

Authors are with the Mechanical Engineering Department at the University of Nevada, Las Vegas (UNLV)

The supplement video attached to this paper, also provides a full-video link on YouTube

Financial support for this INSPIRE UTC project is provided by the U.S. Department of Transportation, Office of the Assistant Secretary for Research and Technology (USDOT/OST-R) under Grant No. 69A3551747126 through INSPIRE University Transportation Center (http://inspire-utc.mst.edu) at Missouri University of Science and Technology. The views, opinions, findings and conclusions reflected in this publication are solely those of the authors and do not represent the official policy or position of the USDOT/OST-R, or any State or other entity.

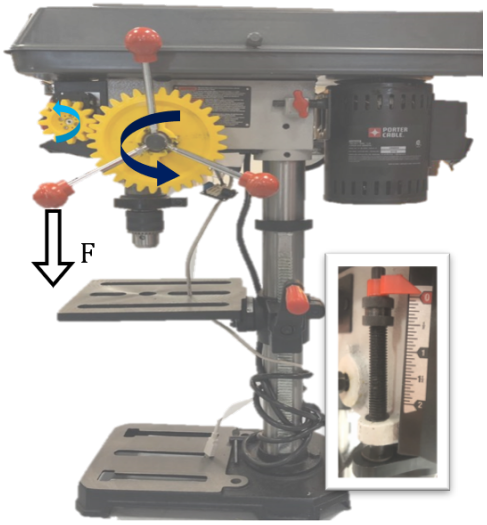

Fig. 2: Customized haptic drill press design; drill chuck position (inset)

concept of using the haptic-based human-in-the-loop aerial drilling.

Toward the-proof-of-concept the paper is structured as follows: Section II describes a customized haptic drill press device and an aerial manipulator concept design; Section III presents criteria for test material selections, and demonstrates the proof-of-concept in the gantry-based testing-and-evaluation platform; Section IV showcases the concept flight trials; and Section V summarizes the results and concludes with future work.

II. Hardware Configuration

A. Customized Haptic Drill Press Design

To provide the operator with haptic feedback, the goal was to render the forces that are transmitted from the drill mounted on the drone. The rationale is that such a design empowers the operator to feel the forces encountered by the drill. Thus, the authors augmented a conventional Porter-Cable drill press with a Dynamixel MX-28 motor (See Figure 2). The augmentation has a single degree-of-freedom rotary handle that drives a drill chuck up and down linearly (0 to 0.05 m). The motor reads the chuck position, senses applied torques, and also generates sufficient stall torque (2.5 Nm at 12 V). It is mounted on the left of the drill press and is linked to the rotary handle by two 3D-printed gears. Both gears are designed to have 0.02 m and 0.06 m radius respectively. The motor senses the torque inputs as the operator rotates the handle while simultaneously provides torque feedback to the operator.

B. Tool Selection and Performance Test

To design a robotic drill manipulator, several hand-drills are considered. The drill press is operated by a binary (on-or-off) power system and the drill chuck motion is linear. The weight of a drone's payload should be considered. Most hand-drills are over 1.5 kg and would require a more complex gripper for the power grasp. Hence Dremel's cordless rotary tool is selected for the manipulator design. This tool is chosen because it provides performances at speeds ranging from 5,000 to 30,000 RPM and has a collet for 7/64" to 1/8" drill bits. Drill performance is demonstrated in Figure 3. Seven materials are selected for experimentation: CAT PS2-10 oriented standard board sheathing plywood (12" x 24" x 7/16); Charlotte 4" diameter PVC pipe (4" x 10" x 1/4"); Simbalux Acrylic sheet (12" x 12" x 1/8"); Hilman weld steel sheet 16GA (12" x 24"x 1/16"); Liftlight Drywall Panel (12" x 12" x 1/2"); Lowe's Concrete Block (5" x 16" x 2"); and Lowe's Red Clay Brick (3" x 8" x 2.25"). Material thickness is considered with the size of drill-bit. DeWalt 7/64" diameter industrial cobalt drill bit (1.5" length) and Bosch 1/8" diameter concrete drill bit (1.5" length) are mounted onto the rotary tool. During experimentation it was observed that the tool could not finish the tasks with concrete and brick (See Attached Video). Hence the rest of materials are used for the proof-of-concept.

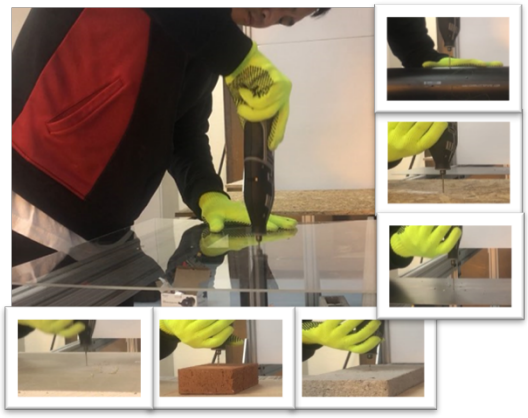

Fig. 3: Selected tool performance test: acrylic sheet, PVC pipe, plywood board, metal sheet, concrete, brick, and drywall (clockwise, inset)

C. Aerial Manipulator Concept Design

A Dynamixel MX-28, is selected as the manipulator for the tool. This tool is attached to the Dynamixel's aluminum joint (See Figure 4a). To mount the drill manipulator, a Powerday S550 hexacopter is selected. The maximum payload is calculated to be 3.6 kg with six 920 kv brushless motors, 9" self-tightening propellers, and a 11.1 V 2200 mAh 3S Li-Po battery. The Pixhawk4 is mounted to control the rotorcraft. Finally, the drill manipulator is attached to the underside of rotorcraft. The manipulator is placed under the drone's center-of-gravity to help counter-balance during flight (See Figure 4b). Table I shows the concept aerial manipulator properties.

III. Haptic Drill Press Trials in Mini-SISTR

Mini-SISTR (Systems Integrated Sensor Test Rig), a gantry-based system for emulating drone motion, is addressed in the authors' previous work [13]. This platform provides safe indoor test flight environments (See Figure. 5). For proof-of-concept, the drill manipulator is mounted to the end of the gantry's vertical axis. The operator uses the customized haptic drill press to control the altitude of the gantry

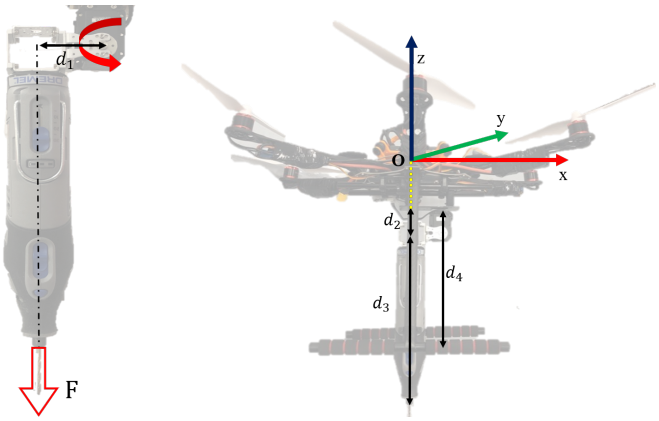

(a) 1 DoF cordless drill manipulator design

(b) Aerial Manipulator Design

Fig. 4: Aerial manipulator with 1-DoF drill manipulator design

TABLE I: Physical Properties of Aerial Manipulator

Symbol	Value	Description
d_1	0.05 m	Length between Dynamixel joint and rotary drill
d_2	0.045 m	Length between drone belly to rotary drill)
d_3	0.29 m	Rotary drill length with a drill bit
d_4	0.21 m	Height of drone's workspace
M_{arm}	0.79 kg	Total mass of 1-DoF drill manipulator
M_{total}	2.79 kg	Total mass of aerial manipulator

manipulator. The Dynamixel mounted on the drill press reads the drill chuck position, and transforms this position into the manipulator's altitude (and thus the rotorcraft's altitude). Forces are sensed when the manipulator contacts selected test materials. The contact pushes the manipulator joint to generate torques. These torques are sensed and converted into forces by dividing with d_1 The forces are transmitted back to the drill press by computer. This haptic integration allows the operator to feel what the drill manipulator is feeling as it contacts the material.

A. Force Rendering Limit for Material Selection

The haptic drill press begins rendering forces when the drill manipulator contacts materials. All materials have properties such as density, shear modulus, and tensile strength. Such properties could impact the amount of generated forces on the drill manipulator. Forces that are over-rendered could damage the system. Hence the force rendering limit is derived from select test materials. First, both Dynamixels on the drill press and the drill manipulator are calibrated, and then a linear regression is performed (See Figure 6). Dynamixel provides a torque sensing value from 0 to 1023, but it is recommended to sense less than the stall torque (2.4 Nm at 12 V) [19]. Therefore the torque sensing value is limited to a maximum 600. As a result, the drill manipulator and the drill press are set to have a maximum force sensing

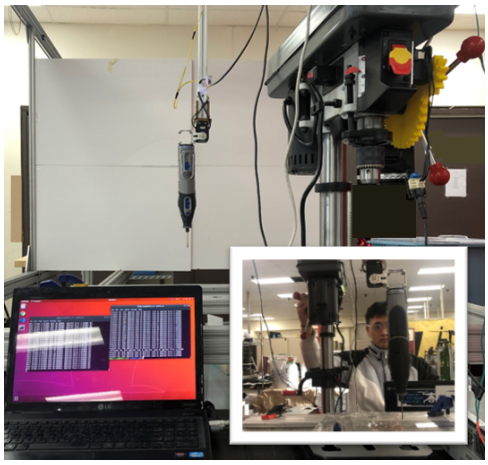

Fig. 5: The haptic drill press (top-right), drill manipulator (background), and operator pressing the drill onto a test material (inset)

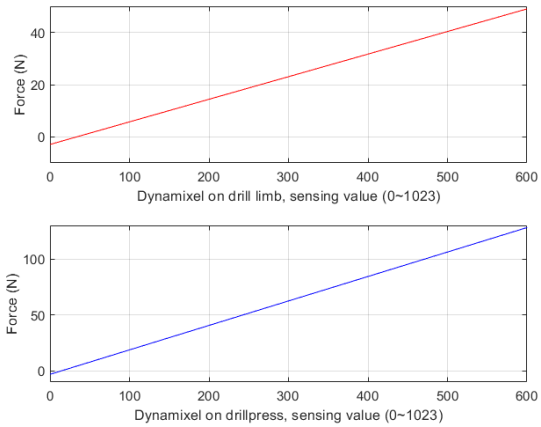

Fig. 6: Dynamixel calibration results: drill manipulator (top) & drill press (bottom)

limit of 48 N, and 127 N respectively. Additionally, the weight of the aerial manipulator is considered. The drill press task is being executed while the rotorcraft hovers, and the drill bit is the only contact point to the test material. Thus the rotorcraft weight was calculated to 27 N. The force rendering limit is summarized as follows:

$$F_{\text{rendered}} < W^{\text{am}} \leq F_{\text{max}}^{\text{dl}} \leq F_{\text{max}}^{\text{dp}} \tag{1}$$

where F_{rendered} is the force rendered from the drill manipulator to the drill press and W^{am}, $F_{\text{max}}^{\text{dl}}$, and $F_{\text{max}}^{\text{dp}}$ are aerial manipulator weight and the maximum force sensing limits of the drill manipulator and the drill press respectively. This force rendering limit enables the operator to select suitable test materials for the proof-of-concept flight trials.

B. Sensitivity

To simulate proper haptic feedback, the varied response of operators due to different body sizes and strength is considered. To capture this response, α is called the sensitivity and is proposed to amplify or reduce the sensed raw force for rendering.

Fig. 7: Haptic drill press on plywood board (left), PVC pipe(Top inset), Acrylic sheet (Bottom inset)

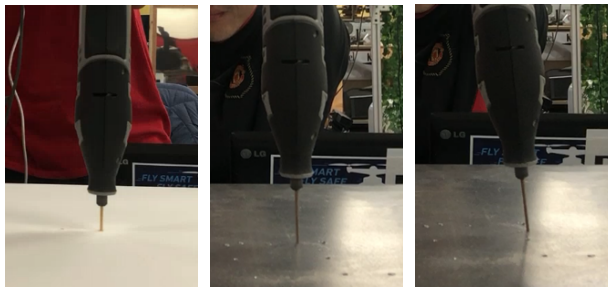

(a) Drywall (F_{raw} Unidentified) (b) Steel sheet (Contact) (c) Steel sheet (Skating)

Fig. 8: Unsuitable materials for haptic drill press

$$F_{\text{rendered}} = F_{\text{raw}} * \alpha \tag{2}$$

where F_{raw} is the initially sensed raw force from the drill manipulator and F_{rendered} is the rendered force to the haptic drill press. This force amplification or reduction assist the operator to distinguish drill press tasks such as initial contact; drill-in; drill-out. This allows the operator to assess material properties to perform drill press tasks. Because the rendered force gives an impact on the drill press system, Equation 1 changes to:

$$F_{\text{raw}} < W^{\text{am}} \leq F_{\text{max}}^{\text{dl}} \tag{3}$$

$$F_{\text{rendered}} \leq F_{\text{max}}^{\text{dp}} \tag{4}$$

In gantry-based and flight trials, the operator tunes α while drilling different materials. This stops when the operator sensitively feels the rendered forces.

C. The Proof-of-Concept in Gantry System

The proof-of-concept trials are conducted using the gantry (Mini-SISTR). Five materials, plywood board, PVC pipe, acrylic sheet, drywall, and rolled steel, are clamped to a test-rig on the gantry for drill press trials (See Figure 7). The operator manipulates the haptic drill press rotary handle in order to control the altitude of the gantry manipulator. The

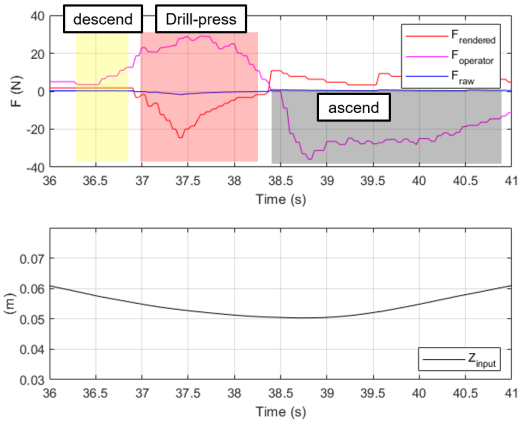

(a) Plywood board

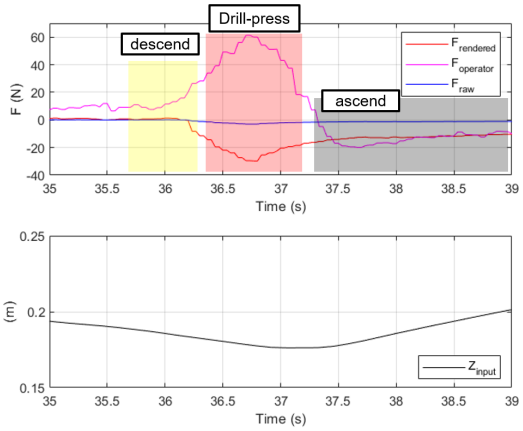

(b) PVC pipe

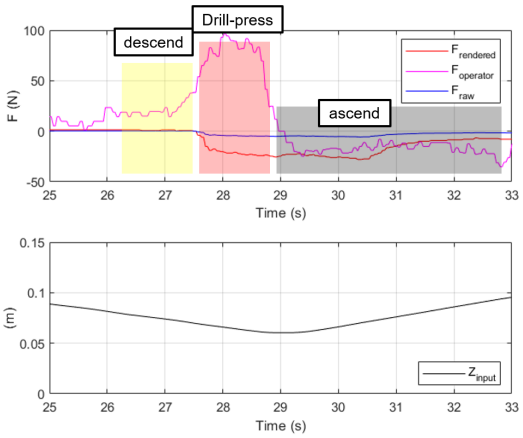

(c) Acrylic sheet

Fig. 9: Haptic drill press in gantry-based system results; Each figure displays force (top) & the manipulator's height (bottom)

gantry then descends the manipulator. When the manipulator contacts a test material, torques are sensed and converted into raw forces using the right-hand rule. The manipulator weight is offset. The offset helps the operator sense forces only by the contacts. F_{raw} is limited to 27 N, low-pass-filtered, multiplied with α, and then rendered to the drill press. α is tuned in the trials, as mentioned in Section III-B. Each

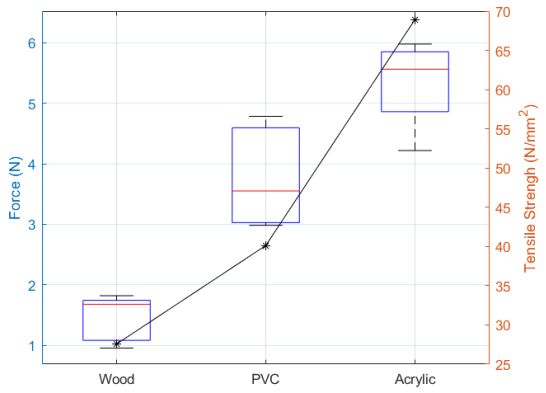

Fig. 10: Haptic drill press in gantry system results summary (raw force value sign changed for better understanding)

of the test materials is drill pressed five times. The drilling speed is set to 30,000 RPM. Figure 8 identifies the unsuitable materials for the trials. The drywall was very easy to drill through, thus F_{raw} was not captured due to low reaction forces. Furthermore, the manipulator was skating on the steel sheet (See supplemental video attached to this paper). It was found that due to the material properties of the steel sheet, a drill press force higher than F_{raw} was required. This violates Equation 3. Thus, the results are addressed with the rest of materials, and these unsuitable materials are ignored in experimentation. In Figure 9, the top graph plots raw forces, rendered forces amplified by sensitivity, and operator input forces. The bottom graph plots the drill manipulator altitude input from the drill press. The operator's force inputs are positive when the manipulator descends. The operator's input increases to counter-act the rendered force while the drill contacts materials. One can also observe that there is existing rendered force after the manipulator is pulled off from materials. This occurred because pull-off task changed the offset. Furthermore, the material tensile strength is found to be proportional to the sensed raw force (See Table II and Figure 10).

TABLE II: Gantry Haptic Drill Press Results Summary

Materials	F_{raw} Mean (N)	F_{raw} Standard Deviation (N)	Sensitivity (α)	Tensile Strength (N/mm^2)
Plywood	-1.4598	0.3907	15	27.57
PVC	-3.7786	0.8374	10	40.13
Acrylic	-5.3287	0.7075	5	68.94

IV. The Proof-of-Concept Flight Trials

The flight trials are implemented for proof-of-concept (see Figure 11). Flight tests serve to verify-and-validate the design performed in mini-SISTR. The operator remote station consists of the haptic drill press, a main computer and a power supply for the dynamixel. The drone's flight environment and workspace are in a motion capture arena. The workspace is two meters away from the remote station, and assembled using Everblock Modular Building Blocks, broadly used in modular construction research [20]. The test materials, plywood board, PVC pipe, and acrylic sheet, are clamped to the workspace for drill press tasks.

For flight stability, the authors updated the aerial manipulator controller that was detailed in [13]. This controller has a proportional-integral-derivative (PID) compensator with anti-windup. The gains are tuned to overcome disturbances from the drill manipulator and errors from the internal estimators (see Figure 12).

Flight trials were conducted five times with each of the materials. Motion capture markers were placed on the workspace to display the target location. The operator first commands the drone to take-off and fly above a target location. This places the vehicle above the materials. The operator then manipulates the drill press rotary handle to descend drone's manipulator to the materials. The forces are sensed when the manipulator contacts on materials. α is tuned in the trials. The operator feels these rendered forces through the drill press. Figure 13 describes flight trial results. Figure 15 displays images from recorded video of the trials. Figure 14 and Table III summarizes the results. One observes the similar plot-form of the results with the ones conducted in the gantry (see Figure 10).

Flight trials ran for 85 seconds. The reaction forces were sensed and rendered between 55 and 65 seconds. The top graph plots raw forces, rendered forces amplified by sensitivity, and operator input forces. The center graph

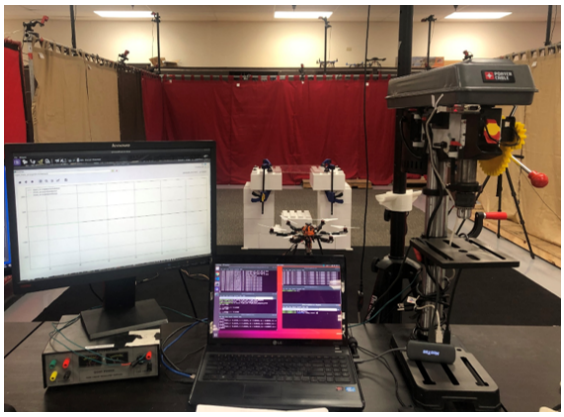

Fig. 11: Flight environment and workspace;

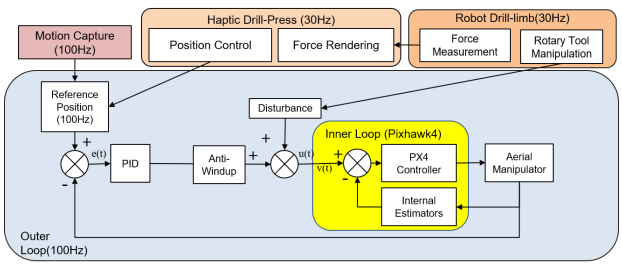

Fig. 12: Overall system scheme

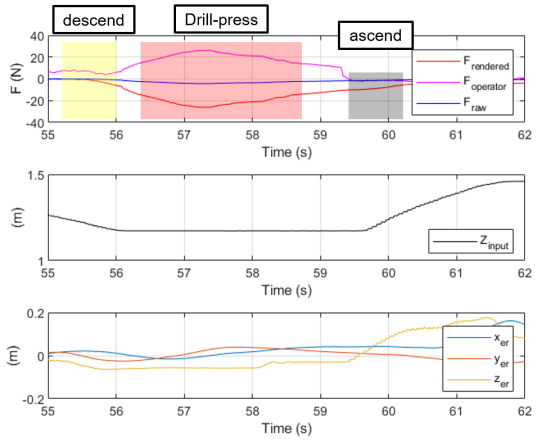

(a) Plywood board

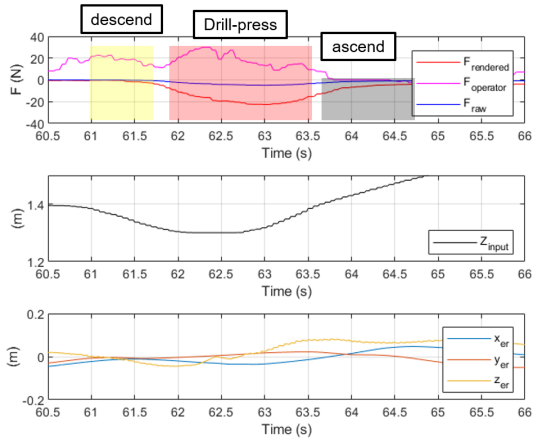

(b) PVC pipe

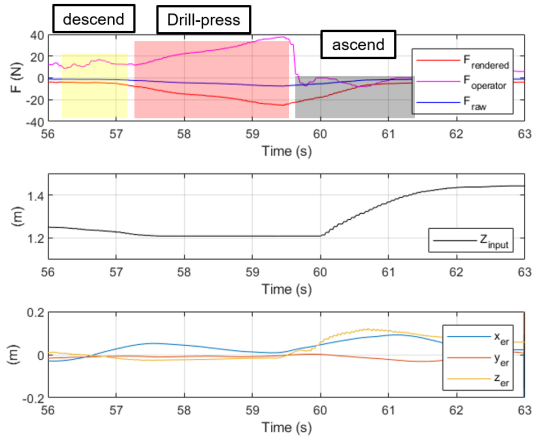

(c) Acrylic sheet

Fig. 13: Flight trial results

plots the rotorcraft altitude inputs from the drill press. The bottom graph plots the position error with respect to the desired position. One also observes that flight fluctuations in drill press, increased the force measurements. Thus the operator reduced α from the gantry to about a half to feel similar forces to the gantry ones through the drill press. (See Table III).

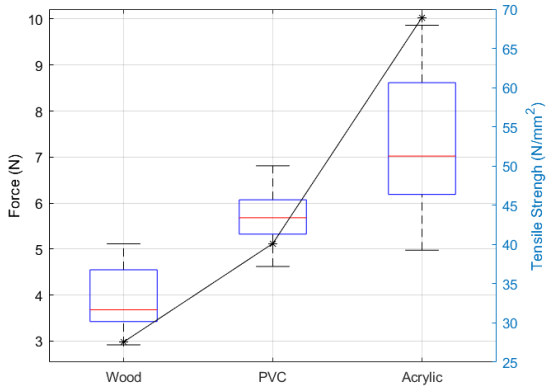

Fig. 14: Aerial drill press test flight results summary (Raw force value sign changed for better understanding)

TABLE III: Aerial Drill Press Test Flight Results Summary

Materials	F_{raw} Mean (N)	F_{raw} Standard Deviation (N)	Sensitivity (α)	Tensile Strength (N/mm^2)
Plywood	-3.93	0.84	6	27.57
PVC	-5.70	0.78	4	40.13
Acrylic	-7.33	1.83	3	68.94

V. Conclusions

In this paper, a concept for haptic-based human-in-the-loop aerial manipulation was presented. The notion is that haptic assessment could enable the operator-in-the-loop to inspect material conditions and increase task dexterity. Drilling was selected as a case study. The authors designed the human-drone interface to remotely drill with a mobile-manipulating drone and a customized haptic drill press. The robotic drill manipulator was fabricated with Dynamixel motor and a commercial rotary tool. Seven materials were originally selected to drill press, but five materials were used for the trials. Force rendering limit was addressed to find suitable test materials, and avoid damages to the system. A parameter, α, was addressed and tuned to amplify or reduce sensed raw forces to render through the drill press. This helps the operator assess material properties to perform drill press collaboratively.

The proof-of-concept trials were conducted in the gantry based testing-and-evaluation platform. In the platform, test materials were clamped, and the drill manipulator was affixed to the gantry vertical axis. The haptic drill press was employed to command the gantry to descend the manipulator. During drill press, α was tuned, and forces were measured and rendered to the operator through the drill press. Figure 8 classified unsuitable materials. Thus results were addressed with the rest of materials (See Figure 9). The test flights were conducted in motion-capture arena. The workspace was built on modular construction blocks. The work materials were clamped to the workspace. The aerial manipulator was deployed for drill press trials. The haptic drill press was used to control drone's altitude. For the trials, α was tuned

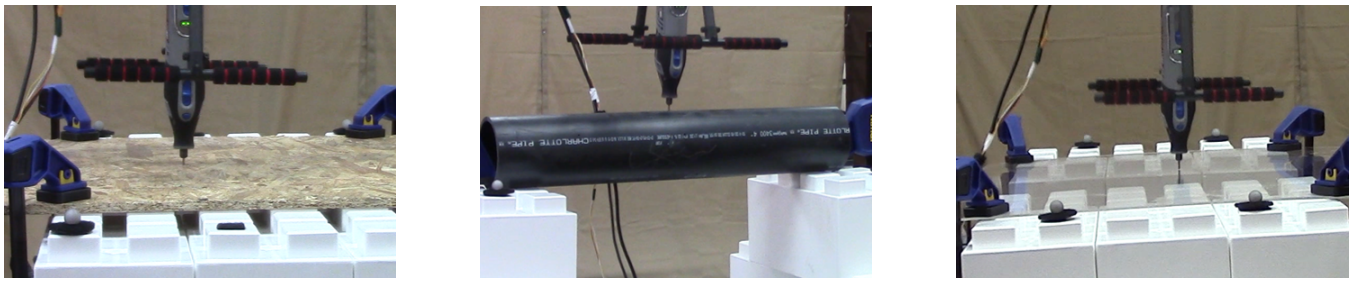

Fig. 15: Flight test closeup view from left to right; Plywood board, PVC pipe, Acrylic sheet

again, and forces were measured and rendered to the operator through the drill press. The results were shown in Figure 9.

Table II and Table III summarized the trial results in the gantry-based platform and test flights. It was observed that material property like tensile strength were related with rendered force and sensitivity. This observation suggested that the operator's handling expertise could be captured with a sensitivity parameter.

The current haptic drill press is based on impedance haptic interface. It corresponds the displacement value with force measurements. By contrast, admittance-based one does the opposite. Transforming the current interface into an admittance-based interface would capture the results more accurately. Impedance feedback controller for drones would increase the quality of tasks. In manipulation tasks, sound, smell, temperature and vision are often overlooked. But these are also important aspects to consider. Hence immersive technologies like augmented reality(AR) and virtual reality(VR), could provide these aspects to dexterously perform aerial manipulation. In the future, similar case study will be demonstrated with these replacements.

REFERENCES

[1] M. Orsag, C. Korpela, S. Bogdan, and P. Oh, "Towards valve turning using a dual-arm aerial manipulator," *IEEE International Conference on Intelligent Robots and Systems (IROS)*, pp. 3411-3416, 2014.

[2] Q. Lindsey, D. Mellinger, and V. Kumar, "Construction of cubic structures with quadrotor teams," *in Proceedings of Robotics: Science and Systems (RSS)*, Los Angeles, CA, USA, 2011.

[3] H-N. Nguyen, S. Park, J. Park and D. J. Lee, "A Novel Robotic Platform for Aerial Manipulation using Quadrotors as Rotating Thrust Generators," *IEEE Transactions on Robotics*, 34(2), p.353-369, 2018.

[4] T. Anzai, M. Zhao, S. Nozawa, F. Shi, K. Okada, and M. Inaba: Aerial Grasping Based on Shape Adaptive Transformation by HALO: Horizontal Plane Transformable Aerial Robot with Closed-Loop Multilinks Structure," *2018 IEEE International Conference on Robotics and Automation (ICRA)*, pp.6990-6996, 2018.

[5] A. Franchi, A. Ollero et al., "The AEROARMS Project: Aerial Robots with Advanced Manipulation Capabilities for Inspection and Maintenance," *IEEE Robotics and Automation Magazine*, 25(4), p. 12-23, 2018.

[6] P. R. Soria, B. C. Arrue, and A. Ollero, "A 3D-Printable Docking System for Aerial Robots: Controlling Aerial Robotic Manipulators in Outdoor Industrial Applications," *IEEE Robotics and Automation Magazine*, 26(1):44–53, 2019.

[7] P. Chermprayong, K. Zhang, F. Xiao, and M. Kovac, "An Integrated Delta Manipulator for Aerial Repair," *IEEE Robotics and Automation Magazine*, 26(1):54–66, 2019.

[8] M. Orsag, C. Korpela, P. Y. Oh, and S. Bogdan, "Aerial manipulation," *Springer International Publishing*, 2018.

[9] N. Enayati, E. De Momi and G. Ferrigno, "Haptics in Robot-Assisted Surgery Challenges and Benefits," *IEEE Reviews in Biomedical Engineering*, vol. 9, pp. 49-65, 2016.

[10] D. Wang, M. Song, A. Naqash, Y. Zheng, W. Xu and Y. Zhang, "Toward Whole-Hand Kinesthetic Feedback: A Survey of Force Feedback Gloves," *IEEE Transactions on Haptics*, 12(2), pp. 189-204, 2019.

[11] HaptX [Online]
Available : https://haptx.com/

[12] P.B. Shull, and D.D. Damian," Haptic wearables as sensory replacement, sensory augmentation and trainer – a review," *Journal of NeuroEngineering Rehabilation*, 12(59), 2015.

[13] D. Kim, and P. Y. Oh, "Testing-and-Evaluation Platform for Haptic-based Aerial Manipulation with Drones," *American Control Conference*, Accepted, 2020.

[14] A. Plowcha, Y. Sun, C. Detweiler, J. Bradlely, "Predicting Digging Success for Unmanned Aircraft System Sensor Emplacement,"*Proceedings of the International Symposium on Experimental Robotics (ISER)*, pp. 153-164, 2018.

[15] Voliro Airborne Robotics [Online]
Available : voliro.com/volab

[16] 3DSystems Touch Haptic device [Online]
Available : https://www.3dsystems.com/haptics-devices/touch

[17] V. Narli, and P. Y. Oh, "Hardware-in-the-Loop Test Rig for Designing Near-Earth Aerial Robots," *International Conference on Robotics and Automation (ICRA)*, pp. 2509-2514, 2006.

[18] K. W. Sevcik, and P. Y. Oh, "Designing aerial robot sensor suites to account for obscurants," *IEEE International Conference on Intelligent Robots and Systems (IROS)*, pp. 1582-1587, 2007.

[19] Dynamixel MX-28 E-Manual [Online]
Available: http://emanual.robotis.com/docs/en/dxl/mx/mx-28/

[20] J. Choi, D. Kim, "A New UAV-based Module Lifting and Transporting Method: Advantages and Challenges," *International Symposium on Automation and Robotics in Construction(ISARC)*, vol.36, pp. 645-650, 2019.

[21] PX4 Controller Diagrams [Online]
Available: https://dev.px4.io/v1.9.0/en/flight-stack/controller-diagrams